scientific reports

Check for updates

OPEN

High-precision monitoring and prediction of mining area surface subsidence using SBAS-InSAR and CNN-BiGRU-attention model

Mingfei Zhu[1,2,3,4,5], Xuexiang Yu[2,3,4,5]✉, Hao Tan[2], Jiajia Yuan[2], Kai Chen[1], Shicheng Xie[1,2], Yuchen Han[1,2] & Wenjiang Long[2]

Coal mining-induced surface subsidence can significantly impact resident safety and hinder regional sustainable development, making precise subsidence monitoring and prediction critical. Existing mining subsidence monitoring technologies often exhibit low spatiotemporal resolution, while subsidence prediction models suffer from heavy dependence on data quality and model assumptions, as well as imprecise parameters. This study addresses these limitations by proposing a novel mining subsidence monitoring and prediction method based on Small Baseline Subset Interferometric Synthetic Aperture Radar (SBAS-InSAR) and the Convolutional Neural Network—Bidirectional Gated Recurrent Unit—Attention (CNN-BiGRU-Attention) model. Focusing on the Banji mining area in Anhui Province, ground subsidence was monitored from July 15, 2021, to September 3, 2023, utilizing SBAS-InSAR technology with Sentinel-1A satellite data. The monitoring results were validated using leveling measurement data. A CNN-BiGRU-Attention prediction model was subsequently constructed based on the time-series monitoring data. The results indicate that the surface subsidence rate in the study area decreases progressively from northwest to southeast, with an average subsidence rate ranging from -49.844 mm/year to -14.810 mm/year. At feature points, the CNN-BiGRU-Attention model effectively captures the characteristics of subsidence time-series changes. For regional subsidence prediction, this model maintains the smallest error, with Mean Absolute Error (MAE) and Root Mean Square Error (RMSE) values of 1.27 mm and 1.44 mm, respectively, and an absolute prediction error of less than 1 mm in most areas. This study integrates SBAS-InSAR technology with the CNN-BiGRU-Attention model to enable unmanned monitoring and prediction of mining subsidence. In comparison to traditional methods, this approach not only reduces monitoring costs but also enhances the accuracy of subsidence predictions, offering critical technical support for the sustainable development of mining areas.

Coal plays a crucial role in the global energy framework. However, coal mining can lead to geological hazards such as surface subsidence, ground fissures, and landslides, posing significant risks to the safety of residents and their property. These hazards also impede the green and sustainable development of affected regions. Consequently, efficient and accurate monitoring and prediction of surface subsidence in mining areas have become prominent research focuses in recent years. Zhu et al.[1] highlighted the geological hazards caused by coal mining, including surface subsidence and ground fissures, which threaten residents' safety and disrupt the sustainable development of mining regions. Hou et al.[2] pointed out that coal mining induces substantial subsidence, creating serious risks to community safety and significantly hindering regional sustainable development, underscoring the need for precise subsidence monitoring and prediction. Xu et al.[3] noted that intensive coal mining activities in the Datong coalfield have resulted in severe geological hazards such as subsidence, ground fissures, and landslides, which pose critical threats to residents and impede progress toward sustainable development.

[1]School of Earth and Environment, Anhui University of Science and Technology, Huainan 232001, China. [2]School of Geomatics, Anhui University of Science and Technology, Huainan 232001, China. [3]Urban 3D Real Scene and Intelligent Security Monitoring Joint Laboratory of Anhui Province, Huainan 232001, China. [4]Key Laboratory of Aviation-Aerospace-Ground Cooperative Monitoring and Early Warning of Coal Mining-Induced Disasters of Anhui Higher Education Institutes, Anhui University of Science and Technology, KLAHEI (KLAHEI18015), Huainan 232001, China. [5]Coal Industry Engineering Research Center of Mining Area Environmental And Disaster Cooperative Monitoring, Anhui University of Science and Technology, Huainan 232001, China. ✉email: ustayxx@163.com

Interferometric Synthetic Aperture Radar (InSAR) enables precise surface deformation detection by analyzing phase differences in radar signals, offering high spatial resolution and the capability to monitor large areas under any weather or lighting conditions[4]. Small Baseline Subset Interferometric Synthetic Aperture Radar (SBAS-InSAR) enhances the InSAR technique by utilizing time-series analysis with images selected for their small temporal and spatial baselines, thereby reducing noise and improving the accuracy of monitoring slow subsidence and deformation processes[5]. Sentinel-1A, a C-band radar satellite launched by the European Space Agency, provides a high revisit frequency of 12 days, delivering a rich and reliable data source for SBAS-InSAR, making it an ideal platform for long-term, detailed monitoring. While SBAS-InSAR technology provides benefits like high spatial resolution and cost-effectiveness for ground deformation monitoring, it also has certain limitations. It is susceptible to decorrelation in areas with dense vegetation or rapidly changing surfaces. Additionally, atmospheric variations, such as humidity and temperature fluctuations, can disrupt radar signals, reducing accuracy. Furthermore, SBAS-InSAR relies on stable scatterers, which limits its applicability in specific regions.

Diao et al.[6] introduced a novel sub-band InSAR approach to monitor large-scale surface deformation in mining areas. Their method enhanced the precision of deformation measurements by addressing challenges in image registration and reducing phase gradients, thereby providing reliable monitoring results even in conditions of extensive subsidence. Zhu et al.[7] integrated Differential Interferometric Synthetic Aperture Radar (D-InSAR), SBAS-InSAR, and Unmanned Aerial Vehicle (UAV) technologies to monitor surface subsidence at the Banji Coal Mine. By comparing against leveling data, their method significantly improved the precision and reliability of subsidence monitoring results. Pawluszek-Filipiak et al.[8] employed a combination of D-InSAR and SBAS-InSAR techniques to monitor ground subsidence at the Rydułtowy mine, which improved the precision of deformation measurements by integrating the strengths of both methods. Qiu et al.[9] employed SBAS-InSAR and Ensemble Empirical Mode Decomposition (EEMD)-Prophet techniques to track land subsidence along the high-speed railway in inland China, significantly enhancing the accuracy and reliability of monitoring results by decomposing nonlinear settlement time series and combining the predictions of multiple intrinsic mode functions. Fadhillah et al.[10] combined Permanent Scatterer Interferometry (PS) and Distributed Scatterer Interferometry (DS) with machine learning postprocessing to analyze land subsidence at Musan mine. Wang et al.[11] employed SBAS-InSAR with a robust sequential adjustment method and to monitor surface subsidence in a Shanxi coal mining area, significantly enhancing result accuracy and computational efficiency. Xu et al.[3] employed D-InSAR, Stacking-InSAR, and SBAS-InSAR to track ground subsidence at Datong coalfield, revealing that Stacking-InSAR is the most effective method for identifying mining deformation in lush mountainous areas. Chen et al.[12] employed DS-InSAR integrated with the Probability Integral Method (PIM) model and arctangent time function to track ground subsidence at Yineng coal mine, significantly improving monitoring accuracy and demonstrating the effectiveness of backfill mining in reducing subsidence. Xie et al.[13] employed SBAS-InSAR to track ground subsidence at Oyu Tolgoi mine, revealing significant subsidence and its spatial distribution, with maximum cumulative subsidence reaching −742.01 mm, highlighting key drivers such as groundwater variations and active mining operations. Lei et al[14]. employed InSAR technology to monitor surface deformation in coal mining areas, offering detailed data for subsidence prediction and improving the understanding of deformation processes. Huang et al[15]. utilized SBAS-InSAR technology to monitor surface deformation in a complex karst mountainous region, providing valuable insights into subsidence patterns and influencing factors such as slope, precipitation, and vegetation.

Currently, ground subsidence prediction models for mining areas primarily encompass statistical models, physical models, and artificial intelligence models[16–19]. Statistical models predict ground subsidence by analyzing historical data and establishing mathematical relationships. This category includes methods such as time series analysis, regression analysis, probabilistic statistical models, spatial statistical models, and spectral analysis. These models effectively leverage historical data for predictions. Physical models predict ground subsidence by simulating the underlying physical mechanisms. Key factors considered include changes in groundwater levels, geological structures, soil compression, and rock layer deformation. These models are calibrated and validated using actual measurement data, providing a comprehensive understanding of the mechanisms behind ground subsidence. Artificial intelligence models predict ground subsidence by constructing features, training models, and performing regression predictions. These models learn and fit ground subsidence patterns without being constrained by complex geological and hydrological parameters. Zhang et al.[20] constructed a hyperbolic secant subsidence prediction model to accurately estimate surface subsidence in thick loose layer mining areas, achieving a 38% improvement in Root Mean Square Error (RMSE) compared to the probability integral method, thereby enhancing the theoretical foundation for mining subsidence prediction and surface damage assessment. Li et al.[21] monitored and predicted the deformation of residential areas in the Panji mining area using InSAR time series analysis and the Grey Model Support Vector Regression (GM-SVR) model, achieving high-precision deformation predictions and enabling effective disaster warnings. Liu et al.[22] integrated SBAS-InSAR with an attention-based Long Short-Term Memory (LSTM) model to perform time-series analysis and prediction of ground subsidence in mining areas, achieving a correlation coefficient of over 0.97, thereby improving prediction accuracy and addressing spatial and temporal dependencies in subsidence data. Zhao et al.[23] developed a numerical modeling strategy to predict ground surface uplift during the flooding process in excavated coal mining areas under complex geological conditions, considering phases before mining, after mine closure, and during flooding, and validated the model using in-situ measurements from the Oelsnitz abandoned coal mine. Hu et al.[24] combined the WeiBull time function and the Improved Probabilistic Integral Method (IPIM) model with SBAS-InSAR technology to predict dynamic subsidence basins, validated in the Wannian Mine with an error range of 0 to 10 mm. Ma et al.[25] employed InSAR technology and the LSTM algorithm to predict mine subsidence in the Shigouyi coalfield, Ningxia, achieving maximum absolute errors of less than 2 cm and maximum relative errors of less than 6%. Li et al.[26] developed a subsidence prediction method for water-

conducting fracture zones in overlying strata of coal mines using a grey theory model, validated in the Daliuta Coal Mine with high accuracy and reliability. Gu et al.[27] introduced an object-oriented probability integration model to predict mining subsidence, validated its reliability through engineering cases, and demonstrated its application in efficiently predicting surface subsidence. Gidon et al.[28] used a bidirectional LSTM model for real-time landslide detection in Meghalaya, India, demonstrating its effectiveness in accurately predicting landslides based on temporal patterns of environmental factors such as rainfall, groundwater levels, and soil properties. Wang et al.[29] proposed a Variational Mode Decomposition–Sparrow Search Optimization–LSTM (VMD–SSO–LSTM) model for landslide displacement prediction, demonstrating enhanced accuracy by decomposing cumulative displacement and rainfall data, which isolates trends, periodicity, and fluctuations essential for real-time landslide risk assessment.

Despite significant progress in ground subsidence prediction, several issues remain[30–34]. Statistical models, while data-driven and capable of using historical data for predictions, lack a physical and geological foundation. This limitation makes it challenging to handle complex and highly variable data. Additionally, these models are highly dependent on data quality and the assumptions underlying the models. Physical models provide an in-depth understanding of the mechanisms behind ground subsidence and help predict subsidence behavior under different conditions. They offer a strong theoretical basis but require large amounts of precise data. Moreover, the simplifications inherent in these models may not align with real-world conditions, making it difficult to address complex geological conditions and nonlinear subsidence behaviors, thus limiting their application. Traditional artificial intelligence models encounter challenges in feature extraction and capturing temporal dependencies, which hinders their ability to fully leverage the spatiotemporal characteristics of subsidence data. Therefore, accurately predicting mining subsidence necessitates the urgent development of a deep learning model that can effectively extract local features from time-series data, model both long-term and short-term dependencies, and capture key characteristics.

By combining the high-precision surface monitoring capabilities of SBAS-InSAR with the robust time-series prediction abilities of the Convolutional Neural Network - Bidirectional Gated Recurrent Unit - Attention (CNN-BiGRU-Attention) model, this approach effectively addresses the limitations of traditional statistical, physical, and artificial intelligence models in terms of data dependency, prediction accuracy, and the ability to manage complex geological conditions. Consequently, this study proposes a method for monitoring and predicting surface subsidence in mining areas using time-series InSAR and deep learning models. Specifically, the approach employs SBAS-InSAR technology to monitor ground subsidence in the Banji mining area from July 15, 2021, to September 3, 2023. The accuracy of the SBAS-InSAR results is validated by comparing them with leveling measurement data, and the spatiotemporal characteristics of ground subsidence are analyzed. Based on the time-series subsidence monitoring results, a CNN-BiGRU-Attention model is constructed for predicting surface subsidence. The prediction accuracy of this model is then compared with traditional Recurrent Neural Network (RNN) and LSTM models to validate its precision.

Study area and data

The Banji mining area is situated at the junction of Lixin County and Yingshang County in Anhui Province and falls under the administrative jurisdiction of Huji Town, Lixin County. Geographically, it is located between longitudes 116°09′ to 116°30′ E and latitudes 32°51′ to 32°56′ N. The mining area spans approximately 6.0 km from east to west and 4 to 7 km from north to south, covering an area of 33.6 square kilometers. Positioned on the Huai River alluvial plain, the terrain is flat, with the monitored area predominantly comprising villages and farmland. The Banji mining area is geologically situated on the northern flank of the Chenqiao anticline within the Huainan coalfield. The structural framework of the region forms a complex syncline trending northwest-west. As a fully concealed coal-bearing area, the stratigraphic sequence, as revealed by drilling, spans from the Ordovician to the Cenozoic, including the Ordovician, Carboniferous, Permian, and Cenozoic formations. The region experiences a monsoon warm temperate semi-humid climate with distinct seasons, an average annual temperature of 15.1°C, and average annual rainfall of 893.74 mm. Due to space constraints, this study focuses on surface subsidence monitoring and prediction specifically for the Chenzhuang area within the Banji mining area. The area is densely built-up, with significant impacts from coal mining activities. Its stable climate and flat terrain minimize the influence of topographic complexity on data coherence, making it ideal for long-term monitoring studies.

Seven leveling monitoring points were established in the study area, as illustrated in Figure 1. The satellite imagery in figures 1, 4, and 5 was generated using ContextCapture software (version 4.4.10). The software can be accessed at the following URL: https://www.bentley.com/software/contextcapture/. Using third-order leveling measurements, ground subsidence at these points was monitored from July 15, 2021, to September 3, 2023. These measurements were used as true values to validate the SBAS-InSAR monitoring results. The SAR data for this study were obtained from the European Space Agency's Sentinel-1A satellite, comprising 66 SAR images collected between July 15, 2021, and September 3, 2023. Relevant parameters are listed in Table 1. The external DEM used in the study was sourced from the Shuttle Radar Topography Mission (SRTM) with a resolution of 30 meters, which helps to remove terrain effects. Additionally, Precise Orbit Determination (POD) data provided by the European Space Agency (ESA) were used to accurately determine the satellite's position, thereby enhancing the overall accuracy of deformation monitoring. In Sentinel-1A-based deformation monitoring, factors such as terrain complexity, vegetation cover, and atmospheric effects can introduce noise, impacting data coherence and accuracy. To mitigate these challenges, we applied atmospheric delay correction and multi-temporal data processing techniques, minimizing their influence on the monitoring results. Moreover, the study area's flat terrain and dense housing reduce the effects of complex terrain and vegetation, further enhancing data accuracy.

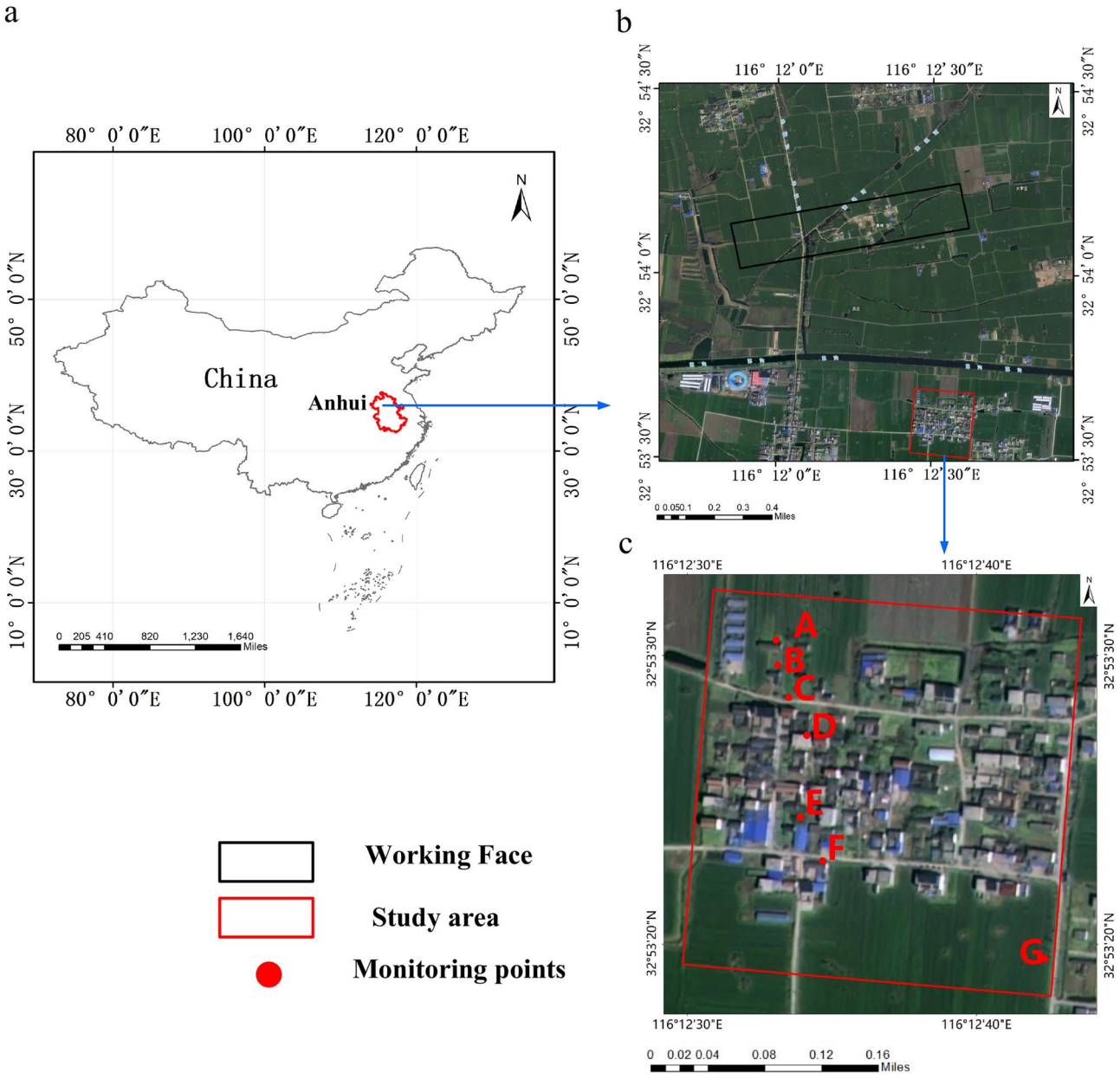

Fig. 1. Overview of the Study Area: (**a**) Shows the geographical location of the study area. (**b**) Shows the relative position of the mining face and the study area. (**c**) The red rectangle indicates the boundary of the study area, and the red dots represent the locations of the monitoring points. The satellite imagery was generated using ContextCapture software (version 4.4.10). The software can be accessed at the following URL: https://www.bentley.com/software/contextcapture/.

Satellite	Data Type	Collection Mode	Wavelength(cm)	Polarization	Orbit Mode	Range Resolution (m)	Azimuth Resolution (m)	Number of Images
Sentinel-1A	SLC	IW	5.6	VV	Ascending	5	20	66

Table 1. Parameters of Sentinel-1A data.

Methods

SBAS-InSAR monitoring technology

SBAS-InSAR technology acquires multiple SAR images of the same area, forming a short-baseline dataset to maintain high coherence between interferometric pairs, effectively mitigating decorrelation due to temporal and spatial baselines[35,36]. After obtaining the cumulative deformation time series, the line-of-sight (LOS)

deformation is converted into vertical deformation, providing the final subsidence monitoring results. The specific data processing steps are illustrated in Fig. 2. Horizontal surface movement in the study area is minimal; therefore, Eq. 1is employed to convert LOS deformation into vertical deformation[1].

$$W = \frac{W_{Los}}{\cos\theta} \tag{1}$$

In this equation, W denotes the vertical component of the satellite's LOS deformation, W_{Los} represents the deformation along the LOS direction, and θ is the radar incidence angle.

Ramirez et al.[37] proposed the selection of a geologically stable reference area based on geotechnical surveys and historical data to ensure the accuracy and reliability of relative deformation measurements, a methodology followed in this study.

In this study, SBAS-InSAR data processing was performed using SARscape Analytics Toolbox (version 5.6.2, https://www.sarmap.ch/index.php/sarscape-analytics-toolbox/), with temporal and spatial baseline thresholds set to 50 days and 2%, respectively. A total of 66 SAR images were acquired from July 15, 2021, to September 3, 2023, forming 195 differential interferometric pairs. These pairs were processed according to the steps shown in Figure 2 to obtain the final surface subsidence time series for the study area.

CNN-BiGRU-Attention prediction model

The CNN-BiGRU-Attention model consists of three key components. First, CNN is used to extract local temporal features from the time-series subsidence data, helping the model identify short-term patterns in the data across different monitoring points. BiGRU processes long-term dependencies in the time-series, allowing the model to consider both past and future subsidence trends, which improves overall prediction accuracy. Finally, the Attention mechanism focuses on the most important time points, assigning higher weight to crucial moments of change, enhancing the model's performance by prioritizing key information. This combination enables the model to effectively capture complex subsidence patterns and make accurate predictions[38]. For example, in a mining area with complex subsidence behavior, CNN detects rapid, localized changes at various monitoring points. BiGRU then tracks long-term trends by incorporating both historical and current data, helping the model recognize gradual, cumulative subsidence patterns. The Attention mechanism highlights moments of sudden change, directing the model's focus to critical shifts, such as abrupt increases in subsidence rate. Together, these components ensure accurate and timely predictions, making the model highly effective in dynamic mining environments.

The CNN component consists of several layers that work together to extract meaningful patterns from the input data. The convolutional layer identifies specific features in the data by computing weighted sums, while activation and pooling layers introduce non-linearity and reduce data dimensions, enabling the network to recognize complex subsidence patterns efficiently. Fully connected layers and normalization are applied to

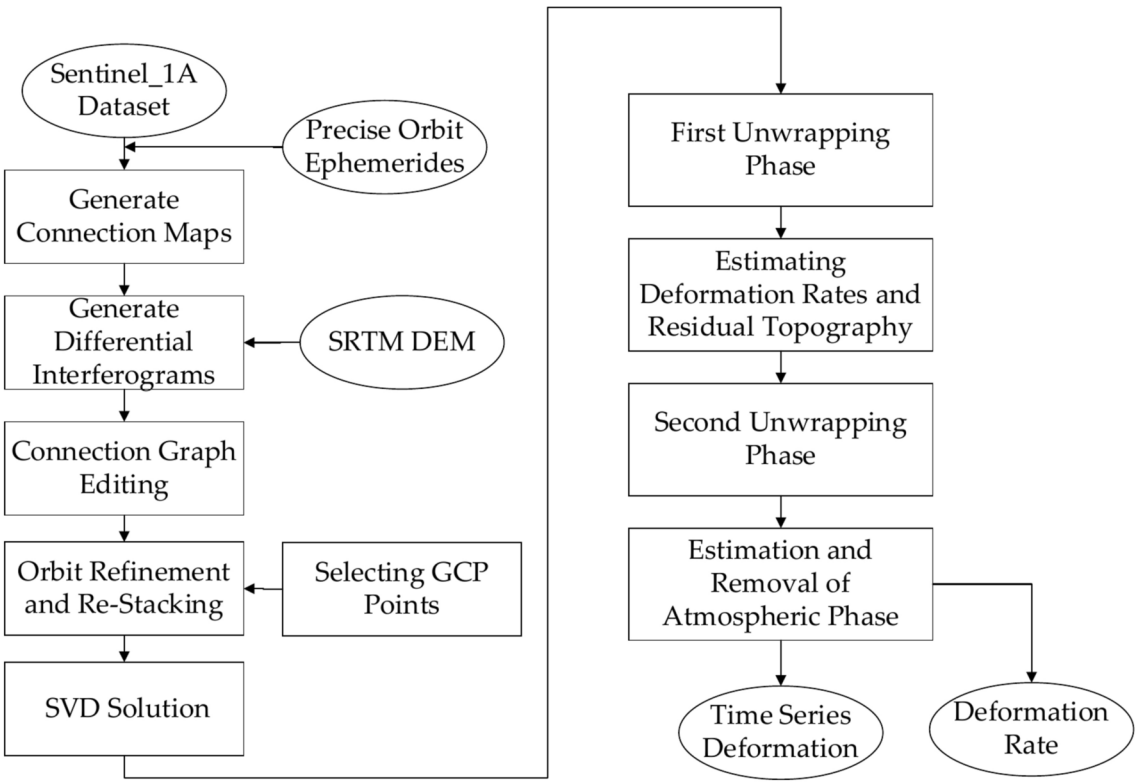

Fig. 2. SBAS-InSAR data processing workflow.

optimize the final predictions, with normalization improving both training speed and model robustness. The main formulas are as follows:

$$(I * K)_{ij} = \sum_{m} \sum_{n} I_{m+i,n+j} \cdot K_{mn} \tag{2}$$

$$P_{ij} = \max(I_{i-m,j-n}) \tag{3}$$

$$O = \sigma(W \cdot I + b) \tag{4}$$

$$\widehat{x} = \frac{x - \mu_B}{\sqrt{\sigma_B^2 + \varepsilon}}, y = \gamma \widehat{x} + \beta \tag{5}$$

In Eq. (2),$(I * K)_{ij}$ represents the value of the output feature map at position (i, j) after the convolution operation.I is the input data,K is the convolution kernel, and i, j and m, n are the position indices on the output feature map and the convolution kernel, respectively. In Eq. (3),P_{ij} represents the value of the output feature map at position (i, j) after the pooling operation. Similarly,m, n are the position indices of the pooling window. In Eq. (4),O is the output,I is the input feature,W is the weight matrix,b is the bias matrix, and σ is the activation function. Equation (5) represents the normalization layer operation, where x is the input data,$\widehat{x}$ represents the normalized input data,μ_B and σ_B^2 are the mean and variance of the current mini-batch data, respectively.ε is a constant for numerical stability, while γ and β are learnable parameters.

The GRU component improves prediction accuracy by regulating information flow through its reset and update gates, which determine the relevant information to retain or discard at each step. This mechanism allows the model to efficiently capture essential patterns in subsidence data over time, considering both previous observations and recent inputs. For example, in predicting subsidence trends, the GRU uses past and current data points to identify consistent patterns, which enhances the model's ability to predict future subsidence accurately.Using the hidden state h_{t-1} from the previous time step and the current input x_t, the GRU model is represented as follows:

$$r_t = \sigma(W_r \cdot [h_{t-1}, x_t] + b_z) \tag{6}$$

$$z_t = \sigma(W_z \cdot [h_{t-1}, x_t] + b_r) \tag{7}$$

where W_r, W_r represent the weight matrices,b_z, b_r represent the bias vectors, and σ denotes the sigmoid activation function. The reset gate r_t determines which information from the previous hidden state h_{t-1} needs to be discarded, while the update gate z_t decides the mixing ratio of the new and old memory.

Next, by calculating the candidate hidden state $\widetilde{h}_t$ and the hidden state h_t, the final output is obtained. The hidden state is then passed to other layers or used as the final output.

$$\widetilde{h}_t = \tanh(W \cdot [r_t \odot h_{t-1}, x_t] + b) \tag{8}$$

$$h_t = (1 - z_t) \odot h_{t-1} + z_t \odot \widetilde{h}_t \tag{9}$$

where W is the weight matrix,$\widetilde{h}_t$ is estimated using x_t and r_t to obtain the possible hidden state. Finally,$\widetilde{h}_t$ and h_t are weighted to get the final state fusion degree,$\odot$ is the Hadamard function.

The BiGRU model improves subsidence prediction by processing data in both forward and backward directions, allowing it to capture complete trend information at each time step. This bidirectional approach enables the model to identify patterns in the data more effectively, which is particularly useful in tracking changes in subsidence over time[39].

The attention mechanism enhances this capability by selectively focusing on important parts of the data. At each time step, it assigns higher weights to critical information, prioritizing key features that may indicate significant changes in subsidence. This helps the model focus on relevant information, making it more accurate in predicting complex subsidence patterns. For example, in a real-world scenario, BiGRU can track subsidence trends in both past and future contexts, while the attention mechanism highlights sudden shifts or critical points in the data, such as areas where subsidence rates rapidly increase. This combination allows the model to better adapt to practical needs in mining areas with varied subsidence behaviors. The specific formulas are as follows (10) - (12):

$$\alpha_{ij} = \frac{\exp(score(h_i, \overline{h}_j))}{\sum \exp(score(h_n, \overline{h}_m))} \tag{10}$$

$$c_i = \sum \alpha_{ij} \overline{h}_S \tag{11}$$

$$\alpha_i = f\left(c_i, h_i\right) = \tanh(W_c \cdot [c_i, h_i]) \tag{12}$$

In the formula,α_{ij} represents the attention score calculated between the encoder output at the j-th time step and the decoder state at the i-th time step.h represents the hidden state at each time step,W represents the weight

matrix associated with the input or hidden state, and α_i denotes the final attention weight obtained through the attention mechanism.

This study uses the CNN-BiGRU-Attention model, as shown in Figure 3, to predict surface subsidence in mining areas. The prediction process involves three main steps: First, data is preprocessed in the CNN layer through convolution and pooling to create feature-rich data vectors. Second, these vectors are passed to the BiGRU layer, which captures both short- and long-term patterns in the data and prevents gradient issues. Finally, the attention mechanism assigns weights to key features, reducing irrelevant information and improving model

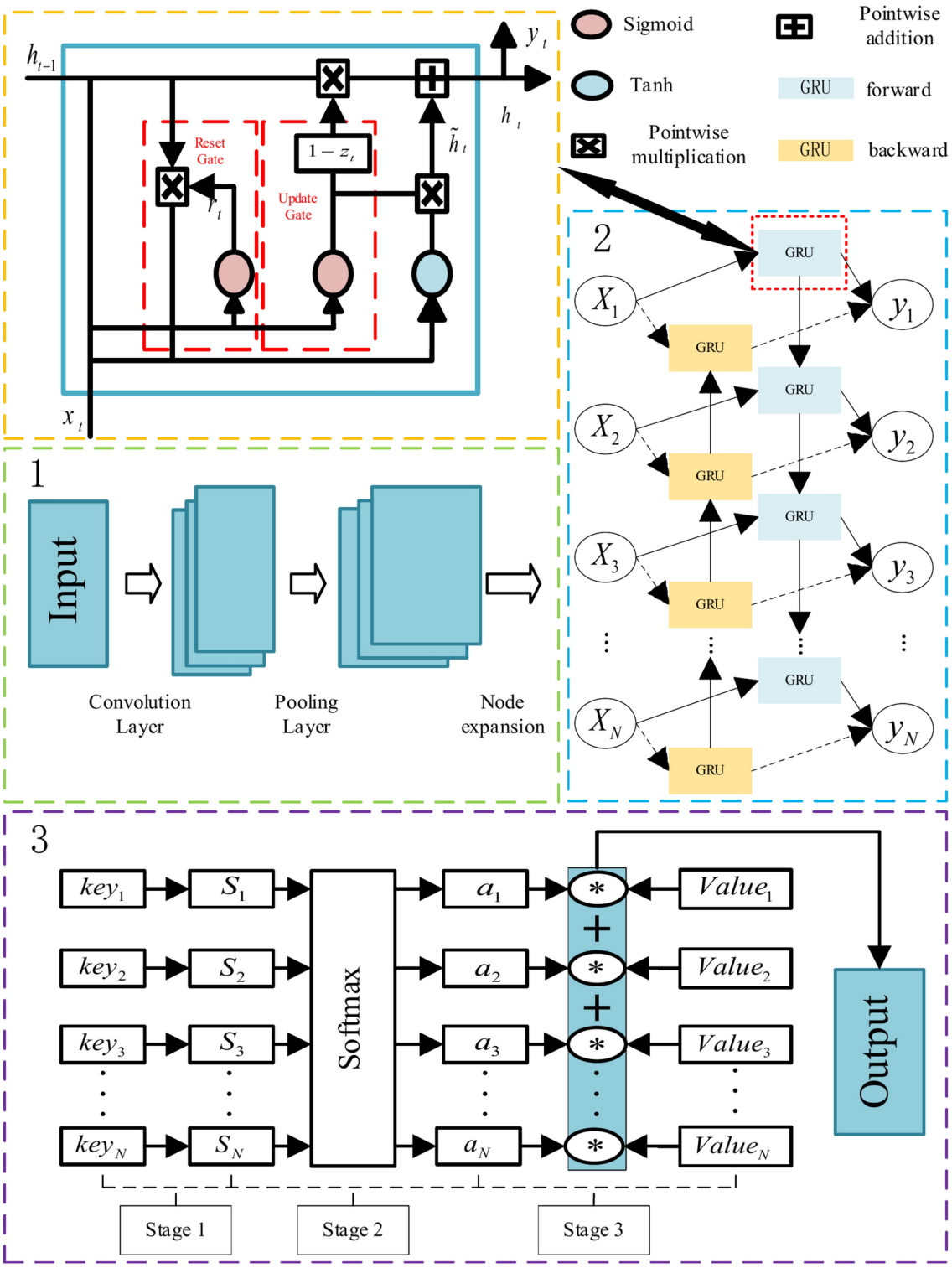

Fig. 3. Principles of the CNN-BiGRU-Attention Model.

efficiency. This process allows the model to focus on essential patterns in subsidence data, resulting in accurate predictions.

Results and discussion

Spatiotemporal characteristics of mining area subsidence

This study employed SBAS-InSAR technology to monitor subsidence in the study area from July 15, 2021, to September 3, 2023. As shown in Figure 4, the coherence values throughout the study area exceeded 0.40, with a maximum of 0.95, indicating overall high coherence. Figure 5 illustrates the vertical subsidence rate within the study area. The northwest region exhibits a higher subsidence rate, peaking at −49.844 mm/year, while the southeast region shows a lower rate, with a minimum of −14.810 mm/year. The higher subsidence rate in the northwest region can be attributed to the location of the active coal mining face in this area. As coal is extracted from the underground mining face, voids are created, leading to surface subsidence directly above these areas. The intensity and extent of subsidence are strongly influenced by the proximity to the mining face, with the northwest side experiencing more significant ground deformation due to the ongoing mining activities concentrated in that region. As the surface subsidence rate diminishes, coherence improves, demonstrating the efficacy of SBAS-InSAR technology in detecting subtle and slow deformations.

Figure 6 illustrates the time series of surface subsidence in the study area from July 15, 2021, to September 3, 2023. The data indicate significant subsidence throughout the region. Since September 2022, the subsidence rate has notably increased, with the affected zone gradually extending from the northwest to the southeast. As of September 3, 2023, the maximum vertical subsidence recorded was −116.110 mm, occurring in the northwest corner of the study area.

In this study, seven monitoring points (A, B, C, D, E, F, and G) were established. Third-order leveling measurements were conducted on July 15, 2021, and September 3, 2023, to calculate the cumulative subsidence at each monitoring point during this period. The results from SBAS-InSAR monitoring were then compared with the leveling measurements to verify the accuracy of SBAS-InSAR monitoring. As shown in Fig. 7, the absolute errors of the SBAS-InSAR monitoring results at points A, B, C, D, E, F, and G are 3.9 mm, 4.1 mm,

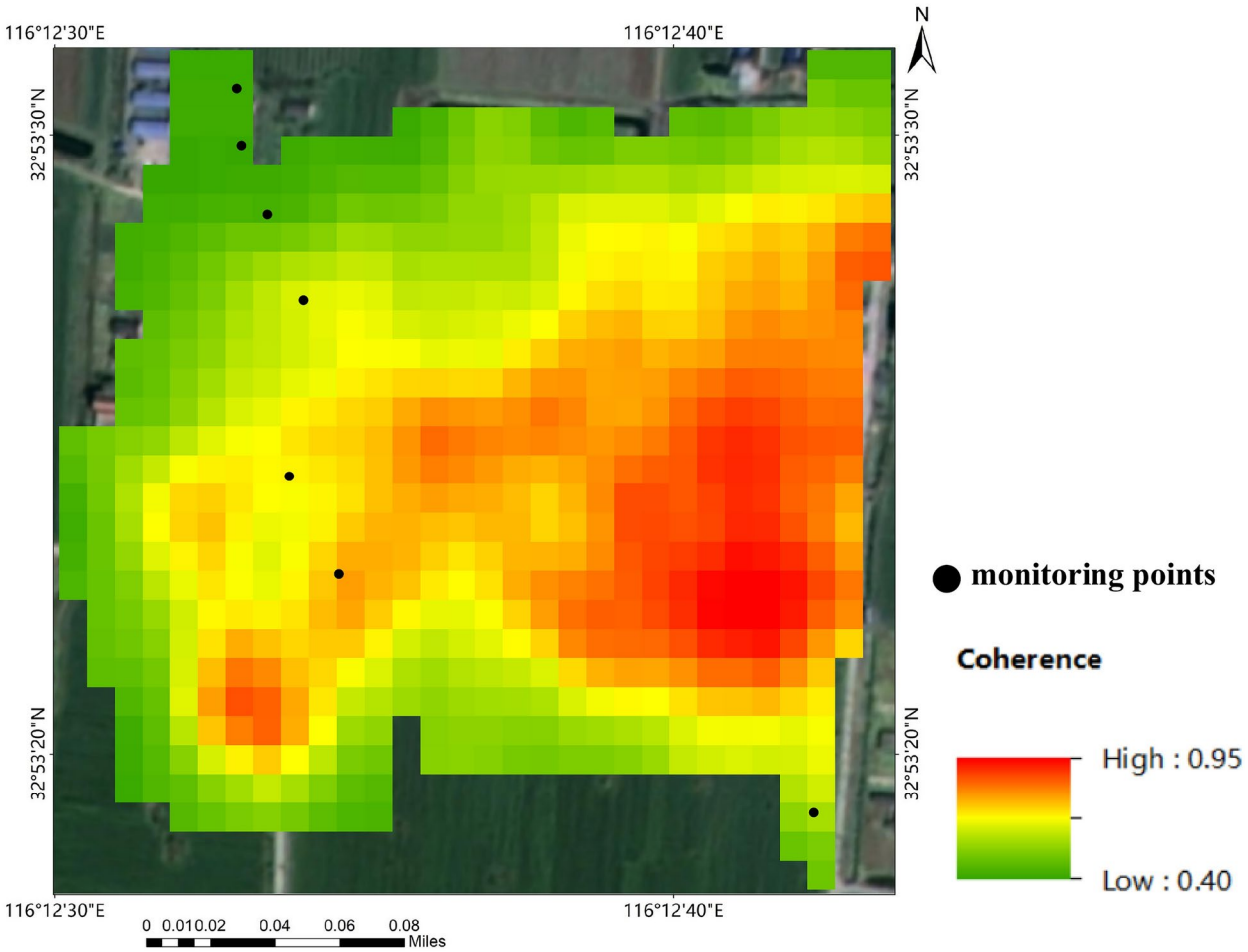

Fig. 4. Coherence map of the study area. The satellite imagery was generated using ContextCapture software (version 4.4.10). The software can be accessed at the following URL: https://www.bentley.com/software/contextcapture/.

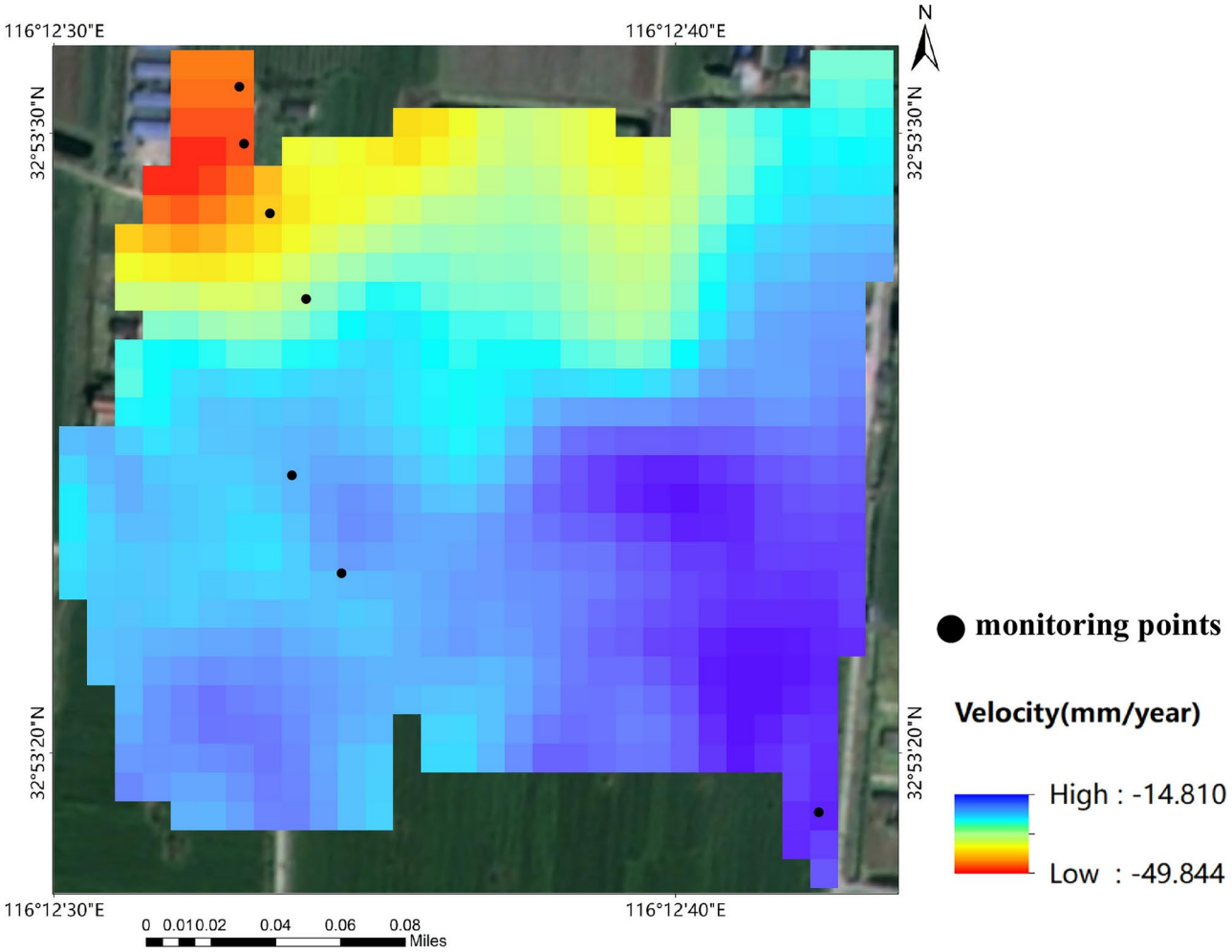

Fig. 5. Annual average surface subsidence rate in the study area. The satellite imagery was generated using ContextCapture software (version 4.4.10). The software can be accessed at the following URL: https://www.bentley.com/software/contextcapture/.

1.4 mm, 1.8 mm, 2.5 mm, 1.3 mm, and 1.2 mm, respectively. The average absolute error is 2.3 mm, and the root mean square error is 2.6 mm. The cumulative subsidence trend observed in Fig. 7 indicates that subsidence at points A to G decreases progressively as the distance from the coal mining face increases, illustrating the reduced impact of mining activities on further monitoring points. The monitoring errors at points A and B, as shown by the higher absolute values in Fig. 7, are relatively larger than at other points. This suggests that SBAS-InSAR is better suited for detecting subtle deformations, especially in areas less affected by immediate mining activity. These findings, as presented in Fig. 7, confirm that SBAS-InSAR monitoring is highly accurate and suitable for studying surface subsidence prediction in mining areas. This clear comparison with leveling results highlights SBAS-InSAR's capability to capture gradual changes across multiple monitoring points.

Figure 8 illustrates the temporal variation in cumulative subsidence at points A, B, C, D, E, F, and G, as monitored by SBAS-InSAR. The data shows a continuous increase in subsidence across all seven points, albeit with varying magnitudes. Points A and B, located in the northwest corner of the study area and in close proximity to the coal mining face, exhibit the highest final cumulative subsidence, exceeding −110 mm. Points C, D, E, and F, positioned in the central region, show subsidence ranging from −38 mm to −100 mm. Point G, in the southeast corner and furthest from the coal mining face, experiences the least subsidence at −32.9 mm.

The cumulative subsidence variation at the seven monitoring points exhibits significant local differences. During the first 380 days of monitoring, the subsidence rates at all seven points were relatively low and stable. After this period, subsidence rates began to increase, with points A and B exhibiting the most significant rise. This increase is attributed to the 110,504 working face of the Banji mining area, located in the northwest part of the study area, which began retreating on July 20, 2022. The retreat intensified surface subsidence in the study area starting in September 2022. The southern monitoring points E, F, and G showed a less noticeable increase in subsidence rates, as they were less affected by the retreating activities of the new working face. The distinct subsidence characteristics observed at these seven monitoring points over various periods render them representative of the subsidence patterns across different regions within the study area. Consequently, these

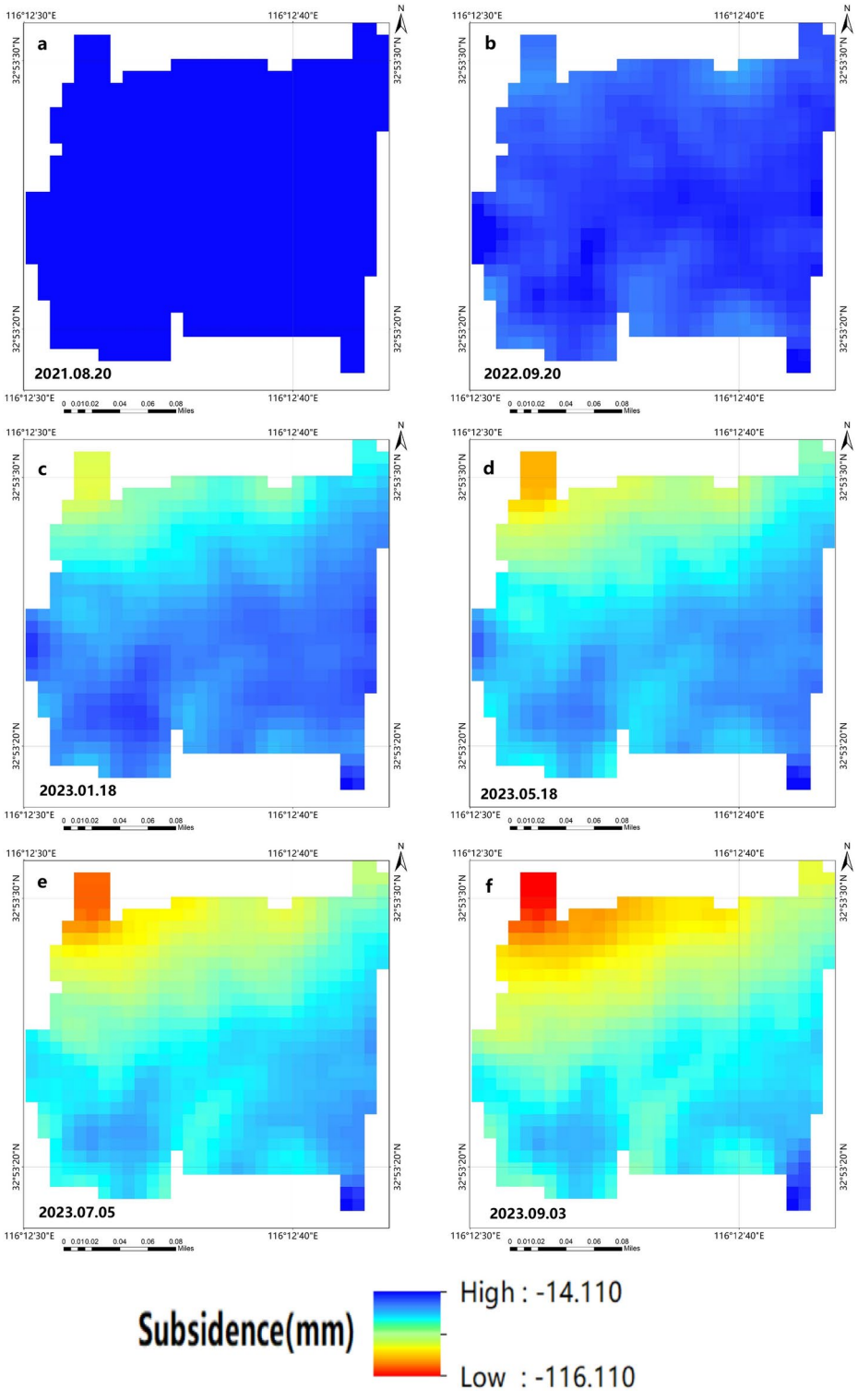

Fig. 6. Spatiotemporal characteristics of surface subsidence in the study area.

seven monitoring points will serve as feature points for the mining area in subsequent sections. This approach enhances the significance of research on subsidence prediction models based on these points.

Prediction and analysis of subsidence at feature points

In this study, we utilized ground subsidence time series data monitored by SBAS-InSAR from July 15, 2021, to May 6, 2023, as our training set. We employed the CNN-BiGRU-Attention model to forecast ground subsidence

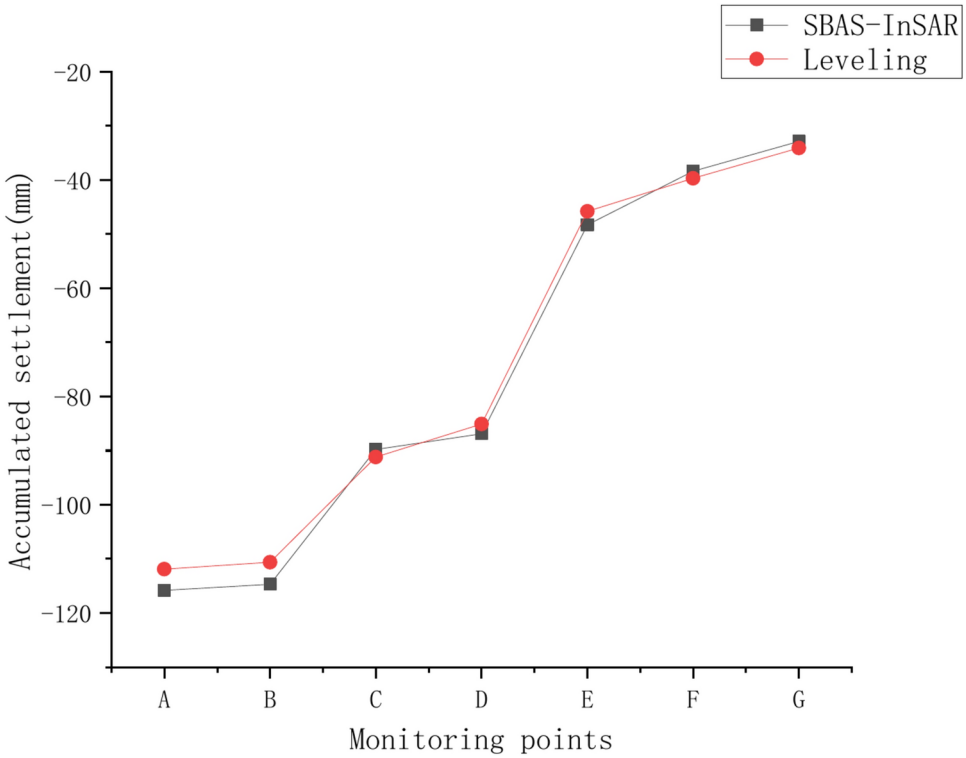

Fig. 7. Comparison of SBAS-InSAR monitoring results with leveling monitoring results at the monitoring points.

at six time points between May 18, 2023, and September 3, 2023. The training-to-forecasting dataset ratio used in this study is approximately 10:1, ensuring sufficient data for model training.

In the CNN component, a 3x3 convolution kernel and a 2-layer convolution structure were selected based on experimental results, which showed that this configuration efficiently extracted local features from the time-series data without significantly increasing computational complexity. A 2x2 max pooling layer was applied to reduce the feature size and prevent overfitting, as experiments with larger pooling sizes led to loss of important temporal features. For the BiGRU component, a 2-layer structure with 64 hidden neurons per layer was chosen after testing different configurations. This structure was found to effectively capture both short-term and long-term dependencies, balancing model complexity and performance. The attention mechanism was set to 4 attention heads, as this configuration performed optimally in focusing on key temporal features, providing a balance between model performance and computational cost.

During model training, the time step was set to 16, and the output length to 1, based on the characteristics of the time-series data and prediction task. The learning rate was selected through grid search, with 0.001 showing the best convergence speed and accuracy. The Adam optimizer was employed to accelerate convergence. A batch size of 32 was chosen after testing different values, as it provided the best balance between training speed and resource utilization. A dropout rate of 0.3 was applied to prevent overfitting, with experiments showing this rate provided optimal training stability. The ReLU activation function was selected to avoid vanishing gradient problems, and MSE was used as the loss function for measuring prediction accuracy.

Mean Squared Error (MSE) was used as the loss function to evaluate the model's performance, with the number of iterations set to 200. After multiple adjustments, the final hyperparameters were determined, as shown in Table 2.

The time series subsidence of seven feature points (A, B, C, D, E, F, G) was predicted using the CNN-BiGRU-Attention model. Figure 9 illustrates the subsidence prediction results for these points, demonstrating that the CNN-BiGRU-Attention model effectively captures local dynamic changes in time series subsidence. Specifically, the model's prediction performance varies across feature points with differing subsidence rates, as shown in the distinct trajectories in Figure 9. For instance, at points A and B (Figure 9a and 9b), where subsidence rates are relatively high, the model effectively tracks the steep decline, closely aligning with SBAS-InSAR measurements. This highlights the model's capacity to handle regions with significant subsidence impacts, likely due to proximity to mining activities. In contrast, at points F and G (Figure 9f and 9g), where the subsidence rate is lower, the CNN-BiGRU-Attention model maintains stable prediction accuracy, even with minimal fluctuations, underscoring its robustness in areas with gradual subsidence changes. Additionally, the attention mechanism within the model allows it to prioritize critical shifts at specific intervals, as reflected in points C and D (Figure 9c and 9d). These points show moderate subsidence rates, and the model successfully emphasizes key time steps where notable shifts occur, resulting in predictions that closely follow the observed data. The model's superior performance over RNN and LSTM models, as shown in Figure 9, underscores its capability to manage both high

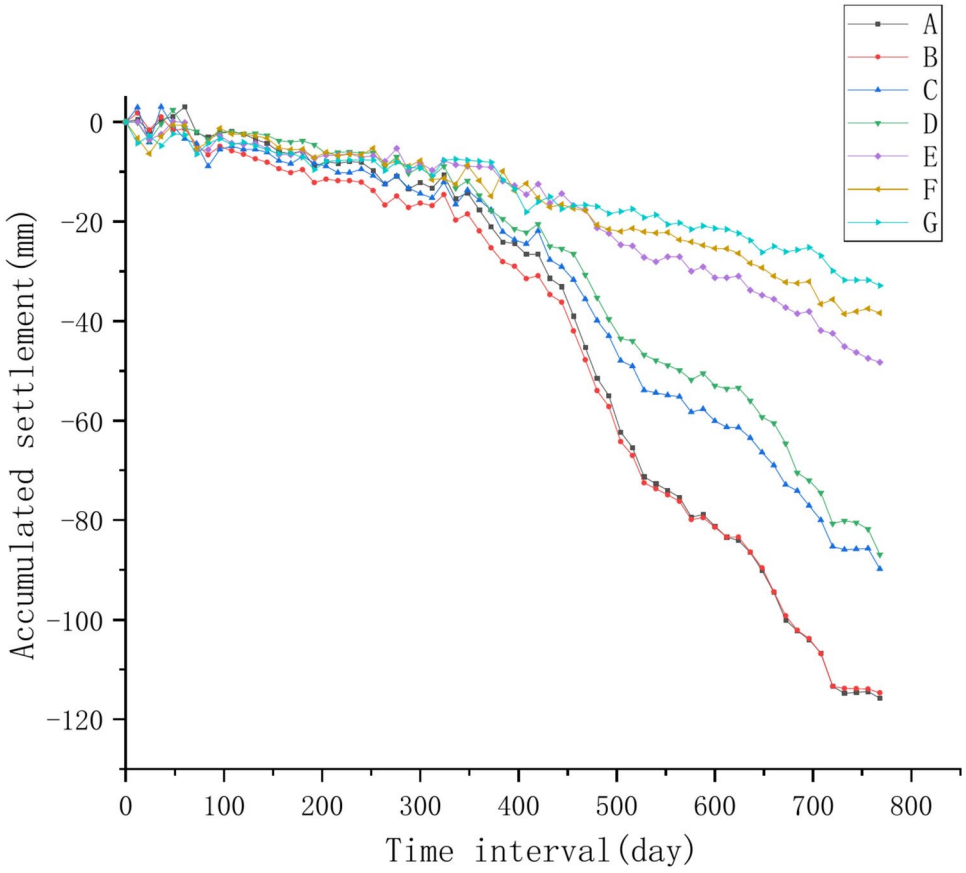

Fig. 8. Time series subsidence of feature points.

Parameters	Setting
Convolution Kernel Size	3×3
Number of Convolution Layers	2
Pooling Type and Size	Max Pooling, 2×2
Number of Hidden Neurons	64
Number of GRU Layers	2
Number of Attention Heads	4
Time Step	16
Output Length	1
Learning Rate	0.001
Optimizer	Adam
Batch Size	32
Dropout Rate	0.3
Activation Function	ReLU
Loss Function	MSE
Epochs	200

Table 2. Model parameters setting.

and low subsidence regions accurately. Overall, Figure 9 illustrates that the CNN-BiGRU-Attention model not only captures diverse subsidence patterns across different points but also adapts effectively to varying subsidence rates, providing a reliable tool for surface subsidence prediction in mining areas.

Table 3 compares the prediction outcomes of the CNN-BiGRU-Attention model with those of the RNN and LSTM models. The comparison reveals that the CNN-BiGRU-Attention model achieves the highest prediction accuracy across all seven feature points and maintains relatively stable accuracy for various subsidence patterns. Notably, at point F, the model achieves the lowest prediction error, with a Mean Absolute Error (MAE) of 0.55

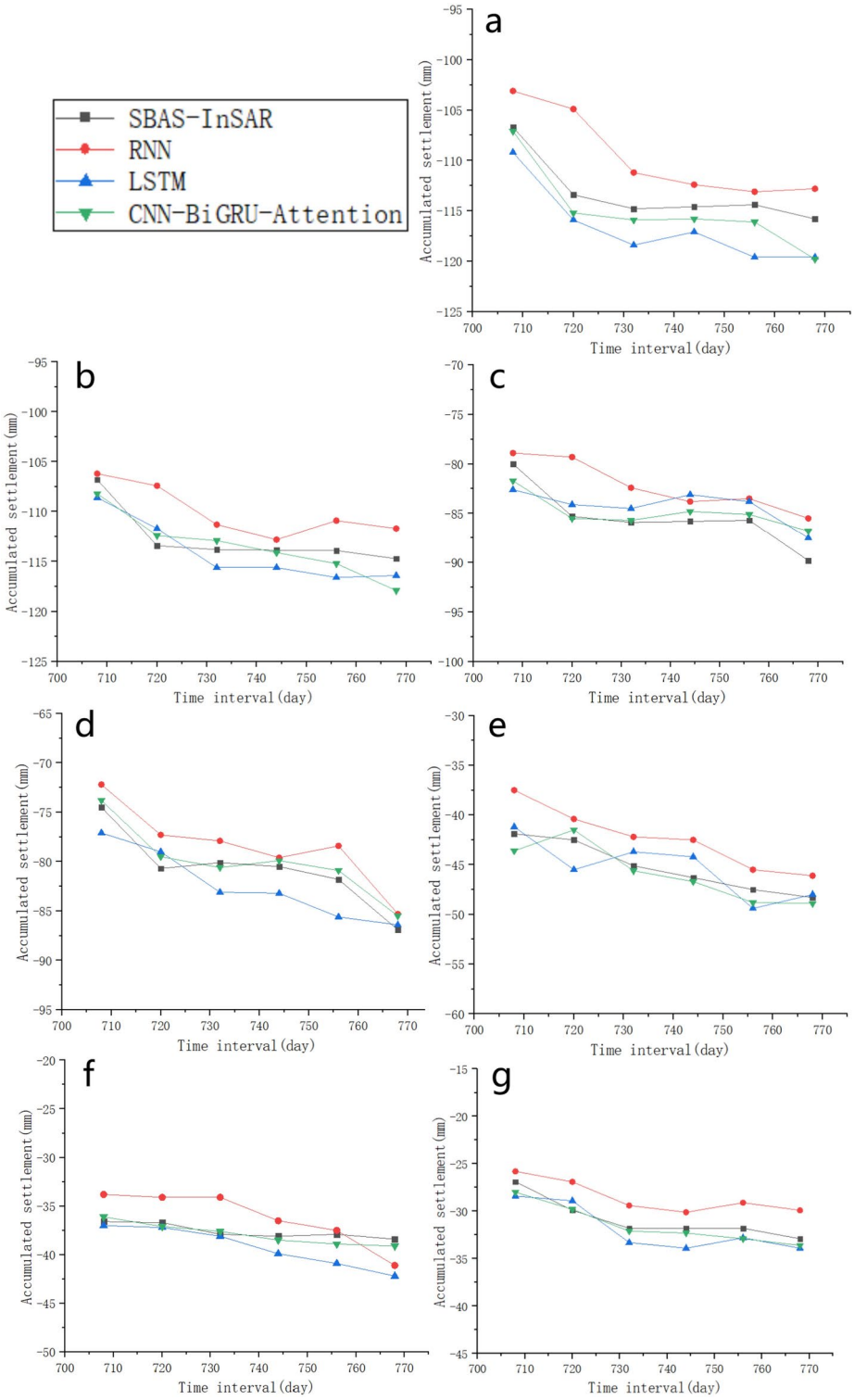

Fig. 9. The time series prediction for feature points A-G. (**a**) Point A; (**b**) Point B; (**c**) Point C; (**d**) Point D; (**e**) Point E; (**f**) Point F; (**g**) Point G.

mm and a Root Mean Squared Error (RMSE) of 0.6 mm. Consequently, the CNN-BiGRU-Attention model demonstrates significant advantages in predicting mining area surface subsidence.

Prediction and analysis of regional subsidence

This study utilizes the CNN-BiGRU-Attention model for time series predictions across the entire study area, comparing its performance with RNN and LSTM models. Model performance is validated using three metrics:

Point	CNN-BiGRU-Attention		RNN		LSTM	
	MAE/mm	RMSE/mm	MAE/mm	RMSE/mm	MAE/mm	RMSE/mm
A	1.70	2.04	3.70	4.35	3.35	3.49
B	1.34	1.62	2.69	3.21	1.91	1.94
C	1.12	1.49	3.18	3.58	2.02	2.10
D	0.88	0.94	2.30	2.47	2.38	2.60
E	0.92	1.03	2.90	3.04	1.57	1.81
F	0.55	0.60	2.32	2.55	1.62	2.13
G	0.63	0.74	2.32	2.42	1.35	1.41

Table 3. Prediction accuracy of feature points.

Model	MAE/mm	RMSE/mm	Time/minutes
RNN	2.76	3.12	7.2
LSTM	2.59	2.97	7.8
CNN-BiGRU-Attention	1.27	1.44	8.9

Table 4. Comparison of regional subsidence prediction results.

MAE, RMSE, and prediction time, as presented in Table 4. The results show that regional subsidence predictions using the CNN-BiGRU-Attention model achieve an MAE of 1.27 mm and an RMSE of 1.44 mm, which are considered very low in the context of mining subsidence prediction. Typically, maximum surface subsidence in mining areas can reach several meters, with subsidence basin boundaries often defined at a threshold of 10 mm. Achieving millimeter-level accuracy demonstrates that the model is highly effective in capturing even subtle surface deformations. This model demonstrates high prediction accuracy for feature points with varying subsidence patterns and excels in regional subsidence predictions, highlighting its effectiveness and reliability in forecasting mining area surface subsidence.

The superior performance of the CNN-BiGRU-Attention model can be attributed to the integration of the convolutional neural network's local feature extraction capabilities, the bidirectional GRU's ability to model long- and short-term dependencies, and the multi-head attention mechanism's ability to capture key features, significantly enhancing prediction accuracy. The study also optimizes hyperparameter configurations, including convolution kernel size, the number of neurons in hidden layers, the number of attention heads, learning rate, and batch size, through multiple adjustments to ensure optimal model performance. Furthermore, measures such as Dropout and the ReLU activation function are adopted to prevent overfitting, effectively improving the model's generalization ability and stability. However, due to the higher complexity of the CNN-BiGRU-Attention model, it requires longer optimization and adjustment times for model parameters compared to the RNN and LSTM models.

This study predicted cumulative surface subsidence in the study area from July 15, 2021, to September 3, 2023. The results are presented in Figure 10, while Figure 11 illustrates the error distribution of the predictions. As shown in Figure 10, the cumulative subsidence distribution predicted by the CNN-BiGRU-Attention model closely aligns with the SBAS-InSAR monitoring results (Figure 6f), both indicating a trend of subsidence gradually slowing from northwest to southeast. Figure 11 demonstrates that in most parts of the study area, the absolute error of the combined model's predictions is less than 1 mm. Only a small portion of the northwest side of the study area shows an absolute prediction error greater than 3 mm, with the maximum absolute error being less than 5 mm. The 3–5 mm absolute prediction error is mainly concentrated in the northwest side of the study area, where the subsidence rate is high and the subsidence magnitude is large. This is primarily due to the drastically changing subsidence patterns in this region, which increase non-stationarity and noise interference in the time series data, reducing the model's accuracy in capturing complex dynamic features.

Ma et al.[25] monitored surface subsidence in the Shigouyi coalfield, Ningxia, using Sentinel-1A satellite data and evaluated the prediction accuracy of the LSTM algorithm, reporting a maximum absolute error of less than 2 cm. In contrast, this study applied the CNN-BiGRU-Attention model to predict surface subsidence in the Banji mining area, achieving a maximum absolute error of less than 5 mm. This result demonstrates the superior predictive performance of the model and further validates the reliability of the proposed method.

Despite the strong performance of the CNN-BiGRU-Attention model in predicting mining subsidence, several limitations arise from its inherent complexity. First, the model's integration of CNN, BiGRU, and attention mechanisms leads to high computational costs. This complexity may impede efficiency when handling large-scale datasets or real-time prediction scenarios, where rapid processing is essential. In resource-constrained environments, or when timely results are critical, these computational demands may restrict the model's practical applicability. Moreover, the model is prone to overfitting, particularly when the subsidence patterns are relatively simple or when data is sparse. Due to its complexity, the model may 'memorize' noise or insignificant details in the training data, which can result in poor generalization to new datasets. This risk is especially pronounced when data is limited or when surface deformation patterns exhibit little variation. Consequently, while the model performs well on training data, its predictive accuracy may decline when applied to new or unseen data.

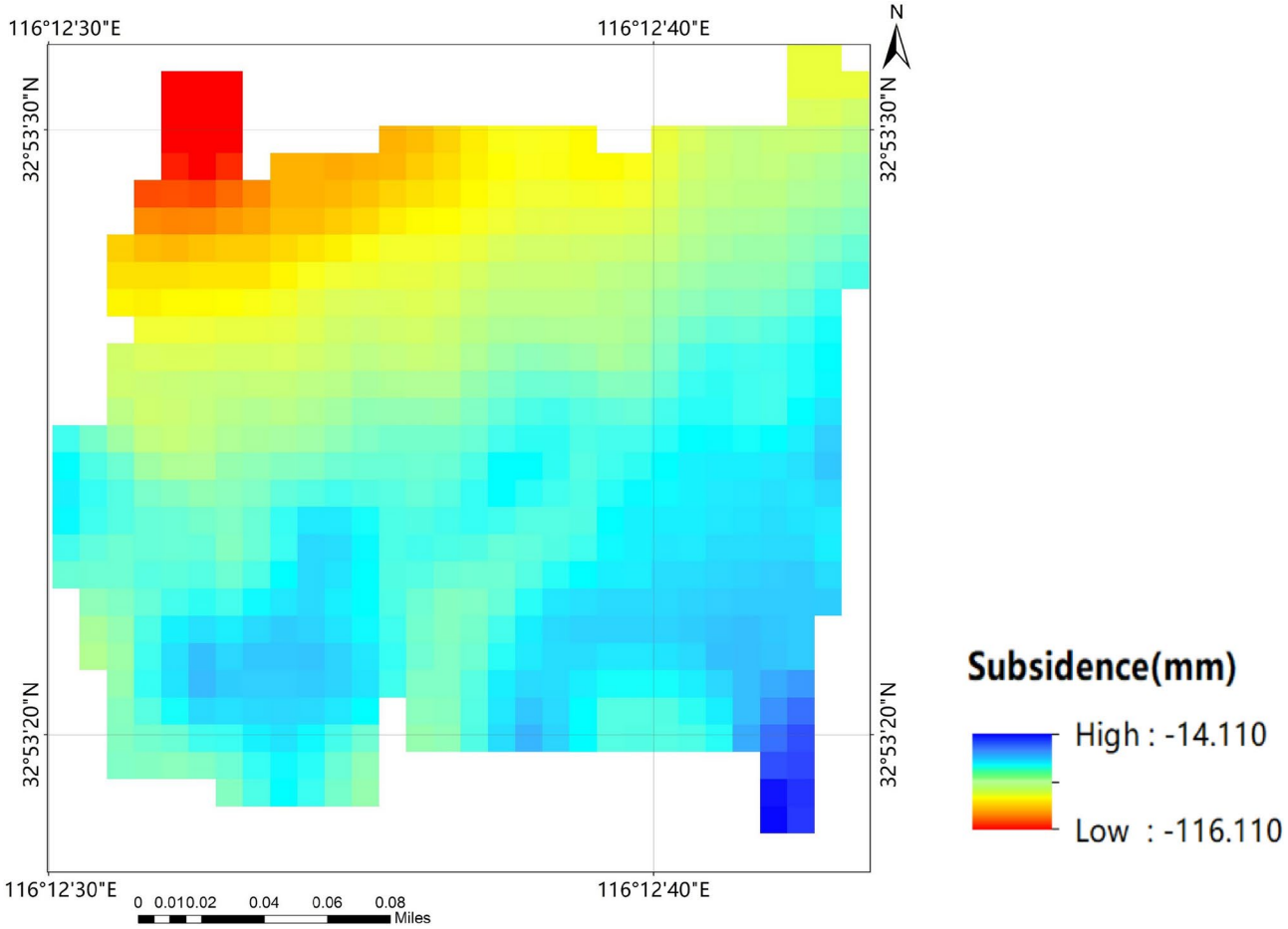

Fig. 10. Predicted results of surface subsidence in the study area on September 3, 2023.

Conclusion

This study utilized Sentinel-1A data and SBAS-InSAR technology to monitor ground subsidence time-series in the study area from July 15, 2021, to September 3, 2023. The monitoring accuracy of SBAS-InSAR technology was subsequently verified using leveling data, and the spatiotemporal characteristics of surface subsidence were analyzed. A CNN-BiGRU-Attention model was then constructed to predict surface subsidence in mining areas based on the subsidence monitoring results. The model's prediction accuracy was validated for both feature points and the overall area.

Results indicate significant surface subsidence in the study area, with the northwest experiencing a higher subsidence rate, peaking at −49.844 mm/year, while the southeast had a lower rate of −14.810 mm/year. The subsidence rate decreased from northwest to southeast, consistent with the mining subsidence patterns influenced by the excavation progress in the northwest.

The CNN-BiGRU-Attention model outperformed RNN and LSTM models in capturing temporal subsidence variations at seven feature points, resulting in the smallest prediction error. The model also demonstrated high accuracy in predicting time-series subsidence for feature points with varying subsidence patterns.

For regional subsidence prediction, the CNN-BiGRU-Attention model achieved MAE and RMSE values of 1.27 mm and 1.44 mm, respectively, surpassing the prediction accuracy of RNN and LSTM models. The absolute prediction error was less than 1 mm in most areas, and in areas with faster subsidence rates, the prediction error remained within 5 mm, demonstrating the model's generalization ability and stability.

The findings of this study can be extended to subsidence monitoring and prediction in other mining areas. The CNN-BiGRU-Attention model demonstrated strong performance in capturing complex temporal subsidence patterns, even in mining areas with challenging geological conditions or significant underground structure variations. By adjusting and training the model to accommodate specific geological parameters, such as hard rock, soft rock, or coal seam thickness, its application can be expanded to various mining environments. Beyond mining applications, this approach holds significant potential for real-time subsidence monitoring by integrating data from GNSS and multi-orbit SAR sources, enabling continuous monitoring and near-real-time predictions. Such a real-time capability is especially valuable for early warning systems, allowing timely interventions in areas at risk of sudden subsidence. Additionally, with further refinement, the model could be adapted to monitor other geohazards, such as landslides and ground fissures, which share time-dependent deformation characteristics.

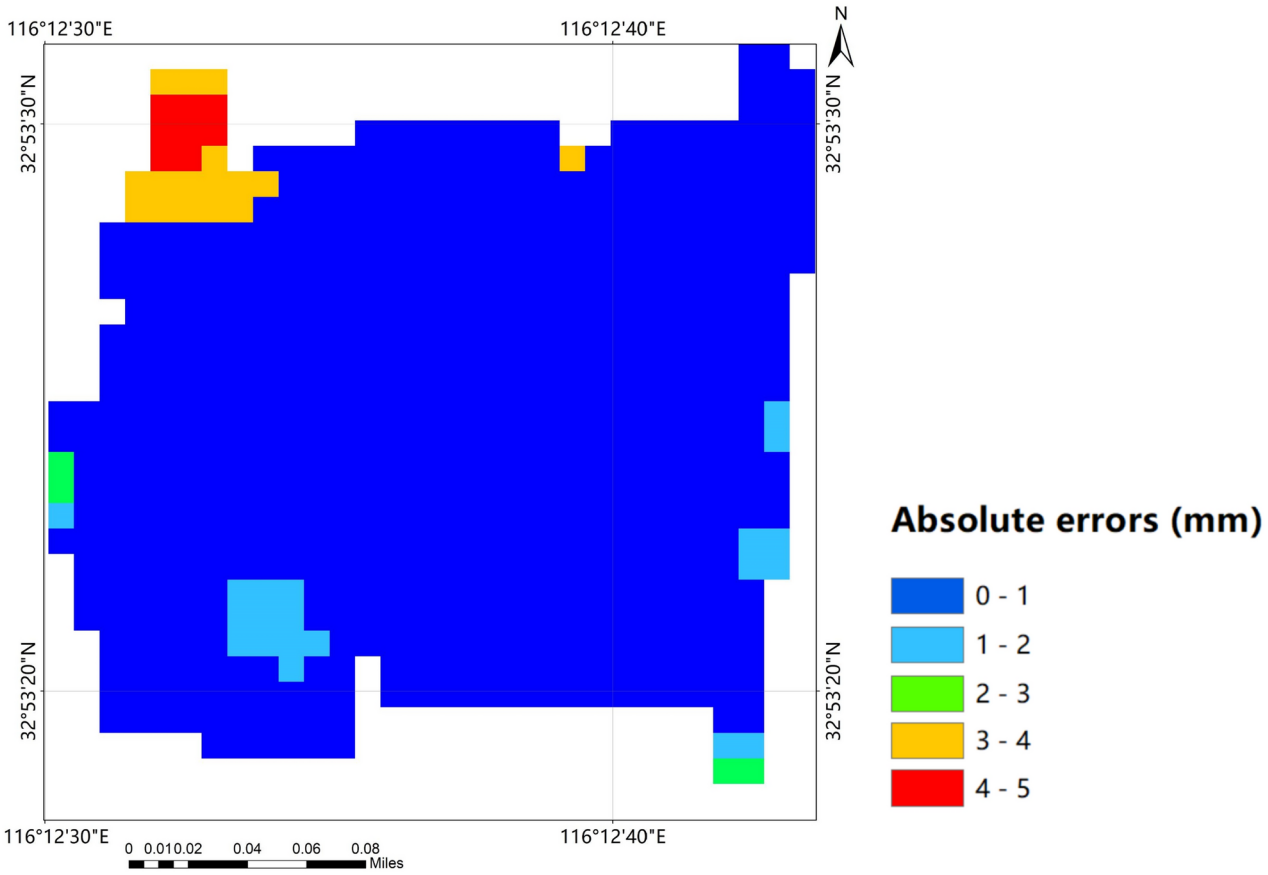

Fig. 11. Error distribution of the predicted settlement amount on September 3, 2023.

This versatility makes the model a promising tool in subsidence and geohazard monitoring, offering timely and accurate predictions essential for risk mitigation across diverse environments.

This study verified the feasibility and effectiveness of using SBAS-InSAR technology and the CNN-BiGRU-Attention model for monitoring and predicting ground subsidence in mining areas. However, certain intrinsic and extrinsic limitations should be acknowledged. Intrinsically, the reliance on single-orbit SAR data may limit the accuracy of vertical deformation measurements, and the limited leveling data restricts comprehensive time-series comparisons with SBAS-InSAR results. Extrinsically, factors such as atmospheric conditions and terrain complexity could introduce noise into the SAR data, potentially affecting measurement accuracy. Future research will aim to improve the model's robustness and prediction accuracy by integrating multi-orbit SAR data and GNSS measurements, which would enhance spatial and temporal resolution. Additionally, adapting the model to address specific geological conditions—such as fault zones, karst formations, and varied rock types—would make it more versatile for subsidence monitoring in diverse environments. Expanding leveling data collection to more frequent intervals could also facilitate finer-grained comparisons with SBAS-InSAR data. A more comprehensive consideration of mining processes, spatial characteristics, and external factors will further optimize the model's accuracy and adaptability across different geological contexts.

Data availability

The radar data and the Precise Orbit Determination (POD) data were obtained from European Space Agency's (ESA) Sentinel-1A satellite (https://search.asf.alaska.edu/ (accessed on 10 March 2024)). The external Digital Elevation Model (DEM) utilized was derived from the Shuttle Radar Topography Mission (SRTM) (https://earthexplorer.usgs.gov/ (accessed on 10 March 2024)).

Received: 23 July 2024; Accepted: 19 November 2024
Published online: 22 November 2024

References

1. Zhu, M. et al. Prediction parameters for mining subsidence based on interferometric synthetic aperture radar and unmanned aerial vehicle collaborative monitoring. *Applied Sciences* **13**, 11128 (2023).
2. Hou, Z. et al. Dynamic prediction model of mining subsidence combined with D-InSAR technical parameter inversion. *Environmental earth sciences* **81**, 307 (2022).

3. Xu, Y. et al. Research on the applicability of DInSAR, stacking-InSAR and SBAS-InSAR for mining region subsidence detection in the datong coalfield. *Remote Sensing* **14**, 3314 (2022).
4. Wang, R. et al. A novel method of monitoring surface subsidence law based on probability integral model combined with active and passive remote sensing data. *Remote Sensing* **14**, 299 (2022).
5. Eker, R., Aydın, A. & Görüm, T. Tracking deformation velocity via PSI and SBAS as a sign of landslide failure: an open-pit mine-induced landslide in Himmetoğlu (Bolu, NW Turkey). *Natural Hazards* **120**, 7701–7724 (2024).
6. Diao, X., Sun, Q., Yang, J., Wu, K. & Lu, X. A novel deformation extraction approach for sub-band InSAR and its application in large-scale surface mining subsidence monitoring. *Sustainability* **15**, 354 (2022).
7. Zhu, M., Yu, X., Tan, H. & Y[1]uan, J. Integrated high-precision monitoring method for surface subsidence in mining areas using D-InSAR, SBAS, and UAV technologies. *Scientific Reports* **14**, 12445 (2024).
8. Pawluszek-Filipiak, K. & Borkowski, A. Integration of DInSAR and SBAS Techniques to determine mining-related deformations using sentinel-1 data: The case study of Rydułtowy mine in Poland. *Remote Sensing* **12**, 242 (2020).
9. Dongwei, Q. et al. Land subsidence analysis along high-speed railway based on EEMD-Prophet method. *Scientific Reports* **14**, 732 (2024).
10. Fadhillah, M. F. et al. Multitemporal analysis of land subsidence induced by open-pit mining activity using improved combined scatterer interferometry with deep learning algorithm optimization. *Scientific Reports* **14**, 6311 (2024).
11. Wang, Y. et al. Near Real-Time Monitoring of Large Gradient Nonlinear Subsidence in Mining Areas: A Hybrid SBAS-InSAR Method Integrating Robust Sequential Adjustment and Deep Learning. *Remote Sensing* **16**, 1664 (2024).
12. Chen, Y. et al. Revealing land surface deformation over the Yineng backfilling mining area, China, by integrating distributed scatterer SAR interferometry and a mining subsidence model. *IEEE Journal of Selected Topics in Applied Earth Observations and Remote Sensing* **16**, 3611–3634 (2023).
13. Xie, Y. et al. Time-Series Analysis of Mining-Induced Subsidence in the Arid Region of Mongolia Based on SBAS-InSAR. *Remote Sensing* **16**, 2166 (2024).
14. Lei, M., Zhang, T., Shi, J. & Yu, J. InSAR-CTPIM-Based 3D Deformation Prediction in Coal Mining Areas of the Baisha Reservoir. *China. Applied Sciences* **14**, 5199 (2024).
15. Huang, G. et al. Study on surface deformation pattern in mine closure area of complex karst mountainous region based on SBAS-InSAR technology. *Frontiers in Earth Science* **11**, 1353593 (2024).
16. Yang, Z., Li, Z., Zhu, J., Wang, Y. & Wu, L. Use of SAR/InSAR in mining deformation monitoring, parameter inversion, and forward predictions: A review. *IEEE Geoscience and Remote Sensing Magazine* **8**, 71–90 (2020).
17. Han, H., Xu, J., Wang, X., Xie, J. & Xing, Y. Surface subsidence prediction method for coal mines with ultrathick and hard stratum. *Advances in Civil Engineering* **2019**, 3714381 (2019).
18. Ma, J., Yin, D., Jiang, N., Wang, S. & Yao, D. Application of a superposition model to evaluate surface asymmetric settlement in a mining area with thick bedrock and thin loose layer. *Journal of Cleaner Production* **314**, 128075 (2021).
19. Bo, H., Lu, G., Li, H., Guo, G. & Li, Y. Development of a Dynamic Prediction Model for Underground Coal-Mining-Induced Ground Subsidence Based on the Hook Function. *Remote Sensing* **16**, 377 (2024).
20. Zhang, J. et al. Hyperbolic secant subsidence prediction model under thick loose layer mining area. *Minerals* **12**, 1023 (2022).
21. Li, J., Gao, F., Lu, J. & Tao, T. Deformation monitoring and prediction for residential areas in the Panji mining area based on an InSAR time series analysis and the GM-SVR model. *Open Geosciences* **11**, 738–749 (2019).
22. Liu, Y. & Zhang, J. Integrating sbas-insar and at-lstm for time-series analysis and prediction method of ground subsidence in mining areas. *Remote Sensing* **15**, 3409 (2023).
23. Zhao, J. & Konietzky, H. Numerical analysis and prediction of ground surface movement induced by coal mining and subsequent groundwater flooding. *International Journal of Coal Geology* **229**, 103565 (2020).
24. Hu, J. et al. Prediction Method for Dynamic Subsidence Basin in Mining Area Based on SBAS-InSAR and Time Function. *Remote Sensing* **16**, 1938 (2024).
25. Ma, F., Sui, L. & Lian, W. Prediction of mine subsidence based on InSAR technology and the LSTM algorithm: A case study of the Shigouyi Coalfield, Ningxia (China). *Remote Sensing* **15**, 2755 (2023).
26. Li, J., He, Z., Piao, C., Chi, W. & Lu, Y. Research on Subsidence Prediction Method of Water-Conducting Fracture Zone of Overlying Strata in Coal Mine Based on Grey Theory Model. *Water* **15**, 4177 (2023).
27. Gu, Z., Zhao, Y., Gao, R. & Wu, L. Research on the Prediction Model of Mine Subsidence Based on Object-Oriented and Probability Integration Method. *Geofluids* **2022**, 8107024 (2022).
28. Gidon, J. S., Borah, J., Sahoo, S., Majumdar, S. & Fujita, M. Bidirectional LSTM Model for Accurate and Real-Time Landslide Detection: A Case Study in Mawiongrim, Meghalaya. *India. IEEE Internet of Things Journal* **11**, 3792–3800 (2024).
29. Wang, H., Ao, Y., Wang, C., Zhang, Y. & Zhang, X. A dynamic prediction model of landslide displacement based on VMD–SSO–LSTM approach. *Scientific Reports* **14**, 9203 (2024).
30. Zhao, B. et al. Prediction method for surface subsidence of coal seam mining in loess donga based on the probability integration model. *Energies* **15**, 2282 (2022).
31. Liu, S. et al. Analysis of mining subsidence characteristics and deformation prediction considering size parameters and mechanical parameters. *Geofluids* **2022**, 5495509 (2022).
32. Sun, Y., Zuo, J., Karakus, M. & Wang, J. Investigation of movement and damage of integral overburden during shallow coal seam mining. *International Journal of Rock Mechanics and Mining Sciences* **117**, 63–75 (2019).
33. Liu, X. et al. Modelling surface subsidence of coal mines using a bonded block numerical method. *Geomatics, Natural Hazards and Risk* **15**, 2336017 (2024).
34. Zhang, G. et al. Predictable condition analysis and prediction method of SBAS-InSAR coal mining subsidence. *IEEE Transactions on Geoscience and Remote Sensing* **60**, 1–14 (2022).
35. Chen, Y. et al. Accuracy verification and correction of D-InSAR and SBAS-InSAR in monitoring mining surface subsidence. *Remote Sensing* **13**, 4365 (2021).
36. Liu, M., Yang, W., Yang, Y., Guo, L. & Shi, P. Identify landslide precursors from Time Series InSAR results. *International Journal of Disaster Risk Science* **14**, 963–978 (2023).
37. Ramirez, R. A., Abdullah, R. E. E. & Rubio, C. J. P. S1-PSInSAR monitoring and hyperbolic modeling of nonlinear ground subsidence in Naga City, Cebu Island in the Philippines. *Geomate Journal* **23**, 102–109 (2022).
38. Niu, D., Yu, M., Sun, L., Gao, T. & Wang, K. Short-term multi-energy load forecasting for integrated energy systems based on CNN-BiGRU optimized by attention mechanism. *Applied Energy* **313**, 118801 (2022).
39. Wang, S., Shi, J., Yang, W. & Yin, Q. High and low frequency wind power prediction based on Transformer and BiGRU-Attention. *Energy* **288**, 129753 (2024).

Acknowledgements

This research was funded by Anhui Provincial Department of Education Fund, grant number 2023AH051190; Key Research and Development Program of Anhui Province, grant number 202104a07020014; Major science and technology projects of Anhui Province, grant number 202103a05020026; Anhui University of Science and Technology Talent Introduction Research Startup Fund, grant number 2022yjrc26; Coal Industry Engineering

Research Center of Mining Area Environmental and Disaster Cooperative Monitoring(Anhui University of Science and Technology), grant number KSXTJC202207.

Author contributions

Conceptualization, M.Z. (Mingfei Zhu); Data curation, H.T. and M.Z. (Mingfei Zhu); Formal analysis, J.Y. (Jiajia Yuan) and K.C.; Investigation, M.Z. (Mingfei Zhu); Methodology, X.Y. (Xuexiang Yu) and M.Z. (Mingfei Zhu); Supervision, H.T.; Validation, H.T. and S.X. (Shicheng Xie); Visualization, H.T.; Writing—original draft, W.L. (Wenjiang Long) and H.T.; Writing—review & editing, Y.H. (Yuchen Han) and H.T. All authors have read and agreed to the published version of the manuscript.

Declarations

Competing interests

The authors declare no competing interests.

Additional information

Correspondence and requests for materials should be addressed to X.Y.

Reprints and permissions information is available at www.nature.com/reprints.

Publisher's note Springer Nature remains neutral with regard to jurisdictional claims in published maps and institutional affiliations.